

Spinal Growth Modulation With an Anterolateral Flexible Tether in an Immature Bovine Model

Disc Health and Motion Preservation

Peter O. Newton, MD,* Christine L. Farnsworth, MS,* Frances D. Faro, MD,†
Andrew T. Mahar, MS,*‡ Tim R. Odell, BS,* Fazir Mohamad, MD,§ Eric Breisch, PhD,*
Kevin Fricka, MD,¶ Vidyadhar V. Upasani, MD,‡ and David Amiel, PhD‡

Study Design. An immature bovine model was used to evaluate multilevel anterolateral flexible tethering in a growing spine.

Objective. To evaluate radiographic, biochemical, histologic, and biomechanical results of tethered spinal growth.

Summary of Background Data. An anterolateral flexible tether has been shown to create a kyphotic and scoliotic spinal deformity in calves. Subsequent disc health and spinal motion has not been analyzed.

Methods. Four consecutive thoracic vertebral bodies (T6–T9) were instrumented anteriorly in 36 1-month-old calves. Seventeen animals (Tether Group) were instrumented with a vertebral staple-two screw construct connected by 2 flexible stainless steel cables. Nineteen animals (Control Group) were instrumented with 1 vertebral body screw with no connecting cable. After a 6-month survival period, the spines were harvest en-bloc and underwent radiographic, computed tomography, biochemical, histologic, and biomechanical analysis.

Results. On average, $37.6^\circ \pm 10.6^\circ$ of coronal and $18.0^\circ \pm 9.9^\circ$ of sagittal deformity was created in the Tether Group, with significant vertebral wedging toward the tether ($P < 0.001$). Disc thickness decreased significantly in the Tether Group ($P < 0.001$), however, disc wedging was not observed. There was no change in gross morphologic disc health or disc water content ($P = 0.73$). However, proteoglycan synthesis was significantly greater in the tethered discs compared with controls ($P < 0.001$), and collagen type distribution was different with a trend toward increased type II collagen present on the

tethered side of the disc ($P = 0.09$). Tethers significantly increased spinal stiffness in lateral bending and in flexion/extension ($P < 0.05$) without affecting torsional stiffness, however, after tether removal range of motion returned to control values.

Conclusion. Tethering resulted in vertebral wedging while maintaining spinal flexibility. Although changes in proteoglycan synthesis, collagen type distribution, and disc thickness were observed, the tethered discs had similar water content to control discs and did not demonstrate gross morphologic signs of degeneration. Growth modulation is an attractive treatment option for growing patients with scoliosis, avoiding multilevel fusions or brace wear. Strategies for fusionless scoliosis correction should preserve disc health, as adolescent patients will rely on these discs for decades after treatment.

Key words: growth modulation, fusionless scoliosis correction, intervertebral discs health, experimental scoliosis, anterolateral tether, motion preservation.
Spine 2008;33:724–733

Idiopathic scoliosis is a complex, 3-dimensional, spinal deformity of unknown etiology. Asymmetric spinal growth and biomechanical imbalance, perpetuated by the Hueter-Volkman effect, has been postulated as a possible etiology for this progressive deformity.^{1,2} Although various treatment methods have been proposed, only bracing and surgical fusion seem to affect the natural history of idiopathic scoliosis compared with observation alone. However, these 2 options have limitations. Orthotics have been found to merely prevent curve progression despite optimal compliance.^{3,4} To obtain a permanent curve correction, surgical treatments sacrifice spinal flexibility, alter stresses on adjacent unfused segments, and may lead to imbalance problems.^{5–8} Ideally, an option would be available that would permanently straighten the deformity while preserving spinal mobility and long-term function.

Dickson theorized that scoliosis was caused by a lateral rotation of the spine in an attempt to balance sagittal anterior overgrowth.⁹ Mechanical alteration of spinal growth with an “internal brace” placed on the convexity of the curve has been proposed as an attractive alternative to arthrodesis.¹⁰ Various investigators have experimented with spinal growth modulation to either correct spinal deformities^{11,12} or to create deformities in animal models^{13–16}; however, few studies have evaluated the resulting condition of the intervertebral disc and growth plate. Biochemical and histologic analyses of these tis-

From the *Rady Children’s Hospital, San Diego, Children’s Way, San Diego, California; †University of Colorado Health Science Center, Denver, Colorado; ‡University of California, San Diego, San Diego, California; §Department of Orthopedics and Traumatology, Faculty of Medicine, Universiti Kebangsaan Malaysia, Cheras, Kuala Lumpur, Malaysia; and ¶The Anderson Orthopedic Clinic, Arlington, Virginia.

Supported by grants from the Orthopedic Research and Education Foundation, DePuy Spine and the Rady Children’s Hospital Orthopedic Research and Education Fund.

Acknowledgment date: July 12, 2007. Revision date: September 14, 2007. Acceptance date: October 16, 2007.

The device(s)/drug(s) that is/are the subject of this manuscript is/are not FDA-approved for this indication and is/are not commercially available in the United States.

Corporate/Industry and Foundation funds were received in support of this work. One or more of the author(s) has/have received or will receive benefits for personal or professional use from a commercial party related directly or indirectly to the subject of this manuscript: e.g., honoraria, gifts, consultancies, royalties, stocks, stock options, decision making positions.

Supported in part by a grant from the Orthopedic Research and Education Foundation.

Study conducted at Rady Children’s Hospital, San Diego and University of California, San Diego.

Address correspondence and reprint requests to Peter O. Newton, MD, Rady Children’s Hospital, San Diego, 3030 Children’s Way, Suite 410, San Diego, CA 92123; E-mail: pnewton@chsd.org

sues need to be performed to predict their function once the “internal brace” has been removed.

The purpose of this study was to determine if a flexible anterolateral spinal tether could create coronal and sagittal plane deformity while maintaining disc viability and spinal flexibility in a rapidly growing animal model. This study used a double tether construct in the rapidly growing calf spine, and biochemical, histologic, and biomechanical tests were performed after 6 months of growth modulation to evaluate disc health and spinal mobility. It was hypothesized that 6 months of spinal growth modulation in an immature calf model would create a substantial deformity in both planes, compared with sham surgery controls. It was also hypothesized that there would be no difference in the biochemical, histologic, or biomechanical aspects (after tether removal) of the spines in the 2 groups.

Materials and Methods

Thirty-six 1-month old male calves were used in this study. A calf model was chosen to explore spinal growth modulation because the size and anatomy of the vertebrae, discs, and chest closely resemble adolescent humans, while the extremely rapid growth would maximize the potential for spinal deformity created due to growth.

Surgical Protocol

The study protocol was Institutional Animal Care and Use Committee (IACUC) approved. Induction with intravenous propofol (2 mg/kg) was followed by intubation with a cuffed endotracheal tube. Anesthesia was maintained with 1% to 3% volatilized isoflurane. A right-sided thoracotomy between the 7th and 8th ribs was performed. The lung was retracted and the pleura and segmental vessels over 4 consecutive vertebrae (T6 through T9) were cauterized in preparation for instrumentation.

In 19 animals, 1 6.25 mm wide and 30 mm long stainless steel vertebral screw was placed in each vertebral body (Isola, DePuy Spine, Raynham, MA). The screws in this group were not connected by a cable (Control Group). In a second group of 17 calves, a vertebral staple and 2 6.5 mm wide and 45 mm long titanium cancellous vertebral screws were placed with bicortical fixation (Frontier, DePuy Spine, Raynham, MA). Two nontensioned 3/16“ stainless steel cables were placed to connect both sets of screws at all 4 levels and secured with set screws (Tether Group). Of note, the screw implants changed between the Control and Tether Groups. The rapid growth rate present in the bovine model resulted in failure of the single screw-tether construct at the bone-screw interface resulting in screw plowing and pull-out.¹⁴ Therefore, a much more secure method of fixation was used in the experimental group (vertebral staple with 2 screws). During implantation, care was taken to avoid damage to the intervertebral discs and epiphyseal growth plates. All calves survived for 6 months. The thoracic spines were then harvested *en bloc* to include vertebral bodies T5 through T10.

Radiographic Analysis

For each animal, dorsoventral and lateral radiographs of the thoracic spine were taken immediately after surgery and after harvest. Vertebral body height and width, and disc height measurements were performed. Vertebral body and intervertebral

disc growth was calculated between 1 and 7 months of age. The magnitude of coronal and sagittal deformity creation was measured over the instrumented thoracic segments using standard Cobb angle techniques.

Computed tomography (CT) was performed on 11 spines from both the Tether Group and Control Group, including reconstructed coronal and sagittal images from 1 mm transverse slices. Vertebral body heights were measured from mid-coronal and midsagittal images, for each instrumented vertebra (T6 through T9), using either eFilm Lite 1.5.2 or GE AMI-Viewer Lite CD Viewer 2.0 software. All measurements were made from 3 consecutive CT images and averaged. Vertebral body heights (mm) were used to calculate vertebral wedging (°).

Biochemical Analysis

Six control and 6 tethered spines were used for biochemical analysis of the intervertebral disc. Immediately after harvest, vertebral bone on either end of the discs was removed to the growth plate keeping the disc and adjacent epiphyses intact (Figure 1). Proximal (T6–T7) and distal (T8–T9) discs from each spine were split at the midcoronal plane with an osteotome and digital photographs were taken to grade the intervertebral discs using the scheme described by Thompson *et al.*¹⁷

The proximal discs (T6–T7) were used to measure water content. Discs were placed in preweighed airtight specimen containers, weighed, dehydrated overnight using a desiccating system under vacuum, and then reweighed. Percent water content was calculated. The 6 tethered samples were compared with the 6 control samples.

The middle disc (T7–T8) was used for analysis of proteoglycan synthesis (³⁵S-sulfate incorporation) and collagen typing (mRNA gene expression for collagens I, II, and X). Bone was removed from both ends of the disc, leaving the endplates intact. Biopsy punches (3 mm diameter) were used to create a

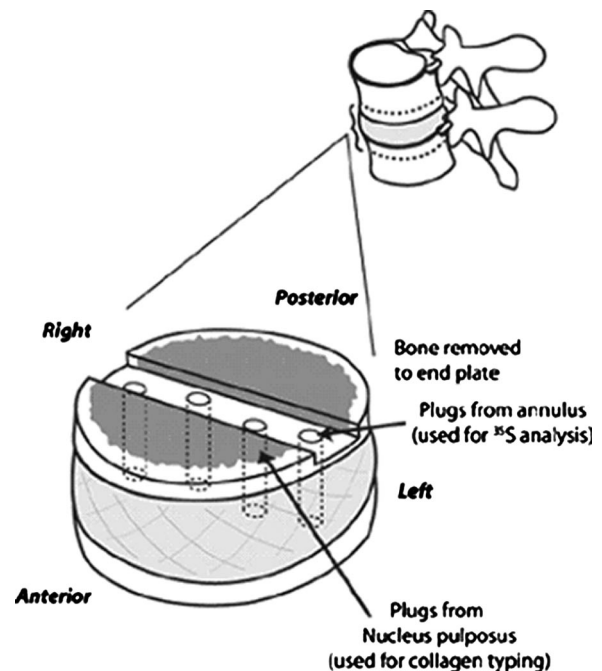


Figure 1. Transverse cross-section of a vertebral body with a central portion of bone removed to the endplate to reveal the disc. Locations that plugs were taken for biochemical analysis are shown.

plug from the annulus on the right and left side at the midcoronal plane of each disc for proteoglycan synthesis analysis (Figure 1). Plugs were immediately placed into tissue culture media containing 5 $\mu\text{Ci}/\text{mL}$ of ^{35}S -sodium sulfate and incubated for 48 hours at 37°C. After extensive dialysis to remove unincorporated sulfate, weighed aliquots of lyophilized tissue were taken for quantitation of incorporated radioactive sulfate by liquid scintillation spectrometry. The results are expressed as counts per minute (cpm) per mg of dry tissue \pm standard deviation.

Additional 3 mm plugs were taken from the T7–T8 disc at the right and left edge of the nucleus at the midcoronal plane and stored at -80°C for semiquantitative reverse transcriptase-polymerase chain reaction (RT-PCR) to determine the relative expression of collagen types. After PCR and agarose gel electrophoresis, band intensities were assessed by NIH image analysis to determine relative amounts of PCR products. Results are expressed as a ratio of the gene of interest to the housekeeping gene, glyceraldehyde-3-phosphate dehydrogenase.

Histologic Analysis

All implants were removed from 6 Control Group and 6 Tether Group spines after harvest. The specimens were fixed in 10% buffered formalin for at least 48 hours and dehydrated using acetone and alcohol solutions. Nondecalcified segments were infiltrated and embedded in methyl methacrylate.^{18,19} The polymerized sections were cut into a single 5 mm thick midcoronal slab,²⁰ ground down to a thickness of 100 μm , and polished to an optical finish (Buehler Inc., Lake Bluff, IL). Each section was stained with Sanderson's Rapid Bone Stain and subsequently with Acid Fuchsin as a counterstain. The remaining discs were decalcified (Decalcifier II by Surgipath), cut to a midcoronal slab and divided via sagittal cuts into right, left, and middle sections of approximately the same width. Each section was embedded in paraffin, cut coronally into 2.5 μm sections, placed on glass slides and stained with hematoxylin and eosin (H&E). Disc thickness and proximal and distal epiphysis thicknesses were measured on the right and left sides and in the middle from digital images of all nondecalcified and decalcified slides (Figure 2). Three measurements were taken at each site and averaged. Intervertebral disc thickness measurements (mm) were used to calculate disc wedging ($^\circ$).

From decalcified sections (Figure 2; 27 control and 27 tethered), microscopic anatomy of the vertebral disc and growth plate were examined for features of degeneration using the grading schemes described by Nerlich *et al* and Weidner and Rice.^{21,22} The following parameters were specifically interpreted as indicators of disc degeneration: neovascularization, granular matrix changes, chondrocyte cloning, and chondro-

cyte cell count. The histologic features of degeneration were semiquantitatively evaluated, ranging between absent (0) and abundantly present (3+) as suggested by Weidner and Rice.²¹ Under 400 \times total magnification, 2 authors counted chondrocyte cell nuclei from 3 fields at the middle of the 9 control and 9 tethered discs. These 6 counts were averaged for each disc.

Biomechanical Testing

Nondestructive testing was performed on 5 control and 7 tethered specimens using a table mounted MTS 858 testing machine (Eden Prairie, MN). For flexion/extension and lateral bending, a cantilever beam method applied moments of ± 4.5 Nm using a displacement control rate of 0.5 mm/s. This setup used a load cell (Sensotec, Canton, OH) and a linear displacement transducer (Space Age Technologies, Ventura, CA) attached to the cantilever beam, as control mechanisms for input moment and calculated angular displacement. For axial torsion, each specimen was mounted in-line with the machine actuator. A 100 N axial load was applied with cyclic moments between ± 2 Nm at an angle control rate of 2° per second.

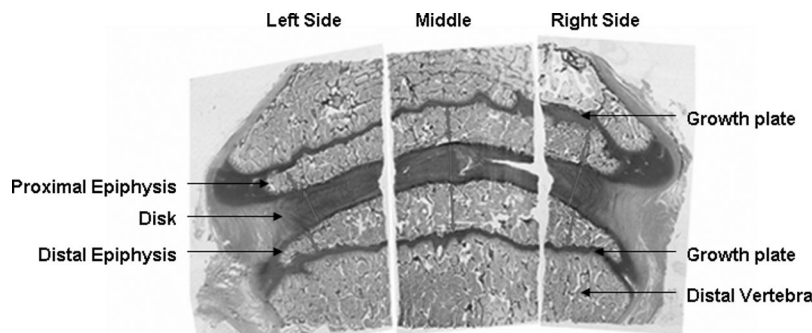
Before mechanical testing, specimens were prepared for kinematic analysis. Kirschner wires (1.5 mm) were inserted in the midline of each vertebral body and parallel to the plane of motion. Four 4 mm reflective markers were then attached to each wire to define a rigid body for each vertebra. Rigid body mechanics were measured using a 4-camera noncontact motion measurement system (Qualisys, AB, Gothenburg, Sweden). Range of motion in flexion, extension, right lateral bending, left lateral bending, right axial torsion, and left axial torsion were then calculated using a custom written kinematic analysis routine in MatLab (Mathworks, Natick MA). The MatLab routine used Euler angle calculation for the plane of motion being tested.

Mechanical data for displacement (mm), force (N), angle ($^\circ$), and torque (Nm) were sampled at 10 Hz for the duration of each test. Kinematic data were sampled at 10 Hz for the duration of each test. As total range of motion was the data point of interest, the mechanical data and kinematic data were not time synchronized. After testing of the control specimens, identical testing was completed on the experimental specimens leaving the tether intact. After this set of testing, the tethers were removed and identical testing repeated. Data for stiffness (Nm/deg) of the entire construct and range of motion ($^\circ$) between the apical vertebrae were reported as average \pm standard deviation.

Statistical Methods

Radiographic measurements (scoliosis, kyphosis, convex *vs.* concave side vertebral body heights, anterior *vs.* posterior vertebral body heights), biochemical (disc water content, ^{35}S up-

Figure 2. Midcoronal section of bovine disc, H&E stained decalcified section. Double arrows show thickness measurements (proximal epiphysis left, middle, and right; disc left, middle, and right; distal epiphysis left, middle, and right).



take, mRNA expression) and histologic measurements (disc thickness, proximal epiphysis thickness, distal epiphysis thickness, cell count) were screened for normality using the normal Q-Q plot of the residuals. If the distribution looked questionable, a more formal check of normality, the 1 sample Kolmogorov-Smirnov statistic was calculated. Levene test for homogeneity of variance was also performed before application of parametric testing.

A series of multivariate analysis of variances or 1-way analysis of variances ($P < 0.05$) were used to compare between-group differences with the independent variable being the presence or absence of the tether. For the biomechanical measures, stiffness (Nm/deg) of the entire construct and range of motion ($^{\circ}$) between the apical vertebrae were compared using a single multivariate analysis of variance with a Bonferroni *post hoc* correction test for multiple comparisons. These multiple comparisons were (1) untethered control *versus* tether intact, (2) untethered control *versus* tether removed, and (3) tether intact *versus* tether removed. Thus, the affect of the tether on spinal biomechanics was evaluated (*post hoc* analysis #1) and the affect of tether removal on restoration of normal mechanics (*post hoc* analysis #2).

■ Results

The Control Group and the Tether Group were similar for initial age, initial mass, and mass after 6-months of growth. The percent mass increase was also not significantly different between the Control and Tether groups ($262\% \pm 56\%$ *vs.* $271\% \pm 49\%$, $P = 0.60$). Out of a reported total blood volume of 2.7 to 3.5 L for calves this size,^{23–25} estimated surgical blood loss was on average less than 20 mL. Of note, surgical time for the Tether Group was significantly longer than the Control Group (84 ± 12 *vs.* 65 ± 17 minutes, $P < 0.001$). The stainless steel tethers were each about 10 cm in length.

Radiographic Analysis

Over 6 months, vertebral body heights in the control group grew an average of $9.7 \text{ mm} \pm 2.0 \text{ mm}$ per level, resulting in a 34% length increase over the 4 surgical levels. Final average vertebral body width was $33.5 \pm 2.5 \text{ mm}$. Control disc thickness increased 100% over these 6 months (from an average of $2.1 \pm 0.2 \text{ mm}$ to $4.0 \pm 0.4 \text{ mm}$). No levering or plowing of screws occurred over the 6-month survival period in any of the Control Group ($n = 19$) specimens. In the Tether Group ($n = 17$), minor screw plowing and levering occurred in all specimens, most pronounced at the proximal and distal screws, however, did not result in clinically significant implant failure.

Immediate postoperative radiographs showed no differences in initial Cobb measurements between the Control and Tether Groups in either the coronal or sagittal planes. After 6 months of growth, the Control Group continued to have essentially no coronal or sagittal deformity ($3.9^{\circ} \pm 3.9^{\circ}$ and $-1.4^{\circ} \pm 3.3^{\circ}$, respectively). Deformities were created in all spines in the Tether Group in both the coronal plane and sagittal plane (on average $37.6^{\circ} \pm 10.6^{\circ}$ and $18.0^{\circ} \pm 9.9^{\circ}$, respectively)

Table 1. Radiographic Parameters for Experimental Groups

	Control ($^{\circ}$) $n = 19$	Tether ($^{\circ}$) $n = 17$	Significance (P)
Initial coronal	0.9 ± 2.2	-0.6 ± 2.1	0.052
Initial sagittal	1.8 ± 3.6	2.3 ± 1.1	0.581
Final coronal	3.9 ± 3.9	37.0 ± 10.5	$<0.001^*$
Final sagittal	-1.4 ± 3.3	20.3 ± 9.3	$<0.001^*$
Coronal change	3.0 ± 4.5	37.6 ± 10.6	$<0.001^*$
Sagittal change	-3.2 ± 4.8	18.0 ± 9.9	$<0.001^*$

Values are mean \pm standard deviation.

Positive coronal values refer to apex left Cobb measurements, negative values refer to apex right Cobb measurements. Positive sagittal values refer to kyphosis and negative refer to lordosis.

*Denotes significant difference between groups.

(Table 1). Figure 3 shows initial and final postoperative radiographs from a representative tethered animal.

CT images showed no evidence of fusion between motion segments and all growth plates remained visible without disruption. Table 2 shows the differences in vertebral body heights and degree of vertebral wedging for the Tether and Control Groups measured on CT in both the coronal (dorsoventral) and sagittal (lateral) planes. Differences are expressed as left minus right side in the coronal plane (positive value indicates untethered side is "taller"), and in posterior minus anterior end in the sagittal plane (positive value indicates untethered side is "taller"). For the Control Group, there was no significant difference in vertebral heights in either the coronal or sagittal plane. In the Tether Group, all 4 vertebrae were taller on the left compared with the right side (total difference of $15.2 \pm 4.9 \text{ mm}$), and taller posteriorly than anteriorly (total difference of $6.0 \pm 3.0 \text{ mm}$).

Biochemical Analysis

There were no gross morphologic differences present between discs evaluated from both the Tether and Control Group. They were all given a Thompson Grade I, as they were white with a bulging gel appearance of the nucleus pulposus. Figure 4 shows a representative control and tethered disc. In addition, water content was not statistically different between the Control and Tether Groups (average \pm standard deviation; $57.1\% \pm 3.2\%$ *vs.* $56.5\% \pm 2.6\%$, $P = 0.73$).

Values for ^{35}S analysis of the Control Group (right- and left-sided values were combined as they were not different), tethered left side, and tethered right side were, respectively, 2125 ± 344 , 3282 ± 318 , and 3097 ± 478 cpm per mg of dry tissue \pm standard deviation. Relative to controls, tethered specimens showed statistically significant increases in incorporation of sulfate on the right ($P < 0.001$) and left ($P < 0.001$) sides indicating a corresponding increase in the rate of proteoglycan synthesis. No differences between the right and left sides of the tethered spines were seen.

Semiquantitative RT-PCR showed that types I, II, and X collagens were expressed in control discs and right and

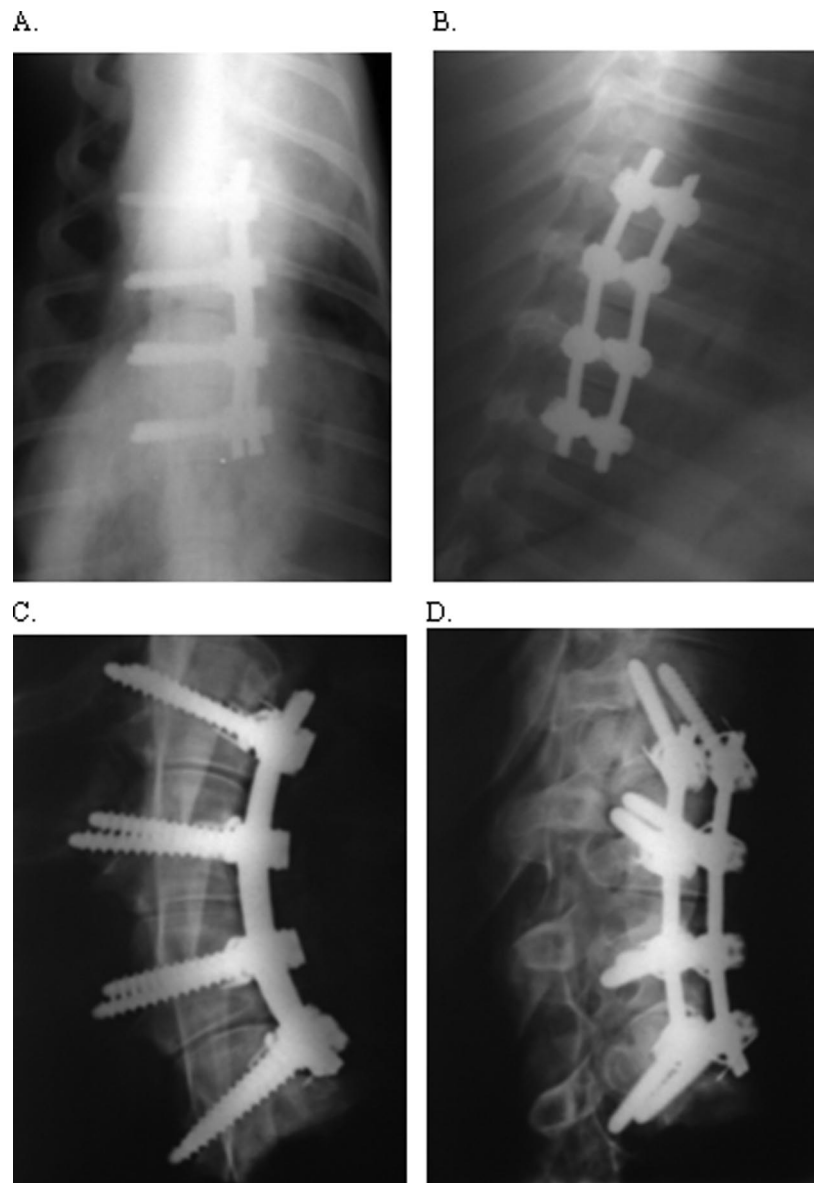


Figure 3. (A) Dorsoventral and (B) lateral initial postoperative and 6 month postoperative (C, D) radiographs from a representative animal from the Tether Group.

left sides of tethered discs. A relatively high standard deviation was observed among specimens in each group possibly as a result of site-specific sampling differences.

Nevertheless, a trend toward an increase in type II collagen mRNA gene expression was observed in the right side of the tethered discs relative to the control disc ($P =$

Table 2. Computed Tomography Vertebral Body Height Differences for Experimental Groups

	Control (n = 11)		Tether (n = 11)		Significance (P)
	(mm)	(°)	(mm)	(°)	
T6 coronal side difference	0.1 ± 0.8	-0.1 ± 1.4	2.0 ± 2.1	3.4 ± 3.6	0.017*
T6 sagittal end difference	-0.1 ± 1.3	-0.2 ± 2.4	-0.2 ± 1.6	-0.3 ± 2.7	0.924
T7 coronal side difference	0.6 ± 1.3	1.3 ± 2.2	5.3 ± 1.9	8.9 ± 3.2	<0.001*
T7 sagittal end difference	0.5 ± 0.9	0.5 ± 1.1	2.3 ± 2.2	4.0 ± 3.7	0.018*
T8 coronal side difference	0.8 ± 1.1	1.4 ± 2.0	5.8 ± 1.5	9.9 ± 2.5	<0.001*
T8 sagittal end difference	-0.2 ± 1.0	-0.4 ± 1.8	3.4 ± 2.2	5.8 ± 3.6	<0.001*
T9 coronal side difference	-0.2 ± 1.3	0.1 ± 2.2	2.1 ± 1.8	3.5 ± 3.1	0.005*
T9 sagittal end difference	0.4 ± 1.1	0.9 ± 2.4	0.4 ± 1.5	0.7 ± 2.6	0.929
Total coronal side difference	1.3 ± 2.7	2.2 ± 4.5	15.2 ± 4.9	25.7 ± 8.2	<0.001*
Total sagittal end difference	0.6 ± 2.6	1.3 ± 4.9	6.0 ± 3.0	10.3 ± 5.0	<0.001*

Values are mean ± standard deviation.

Coronal difference = left side - right side. Sagittal difference = posterior end - anterior end.

*Denotes a significant difference between Control and Tether groups.

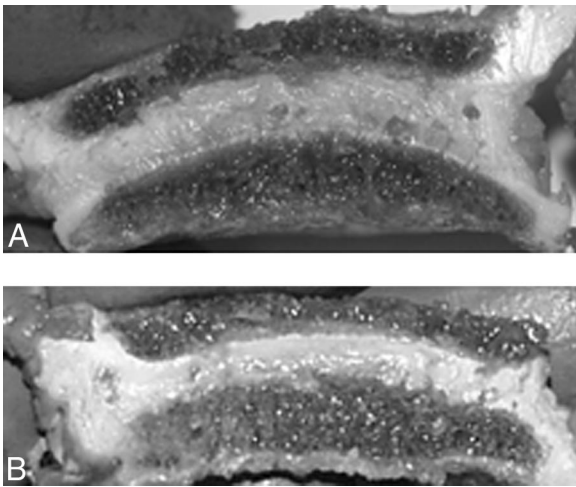


Figure 4. Typical midcoronal sections of a control (A) and a tethered (B) disc. All discs were given a Thompson Grade I.

0.09, Figure 5). There were no other differences in collagen types observed.

Histologic Analysis

There was no evidence of bony bridging across any discs, and all discs remained intact for both groups ($n = 18$ each group). Both proximal and distal epiphyses were present and complete in all slides. The thickness of the proximal epiphysis was decreased, but not significantly, in the Tether Group compared with controls on the left side (2.9 ± 0.5 mm vs. 3.2 ± 0.6 mm, $P = 0.12$), in the middle (3.3 ± 0.5 mm vs. 3.6 ± 0.5 mm, $P = 0.05$) and on the right side (2.9 ± 0.5 mm vs. 3.3 ± 0.6 mm, $P = 0.03$). Additionally, there was no significant difference between the right and left sides for the Tether Group at the proximal epiphysis ($P = 0.87$). The thickness of the distal epiphysis was not altered by the presence of the tether. Disc thickness of tethered spines was decreased on the left side by 27%, in the middle by 21%, and on the right side by 28% compared with the Control Group (left: 3.0 ± 0.4 mm vs. 4.1 ± 0.7 mm, $P < 0.001$; mid: 3.3 ± 0.7 mm vs. 4.2 ± 0.8 mm, $P < 0.001$; and right: 3.1 ± 0.6 mm vs. 4.3 ± 0.7 mm, $P < 0.001$) (Figure 6). There was no difference in disc thickness between the left and right sides in both the Control ($P = 0.26$) and Tether

Groups ($P = 0.35$), indicating no disc wedging in either group.

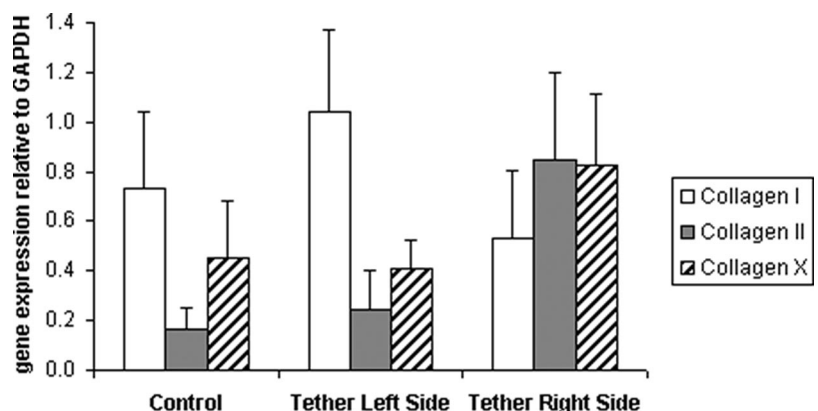
There was no evidence of neovascularization present in any of the control or tethered disc decalcified histologic slides. Granular changes were present in 1 control disc (4%), but not in any of the tethered discs. Chondrocyte cloning was present in 2 of the 27 fields of tethered discs (7%) and 1 of the 27 fields of control discs (4%). Average chondrocyte cell counts were not significantly different between the tethered and control discs (21.3 ± 8.4 vs. 22.5 ± 9.5 , $P = 0.78$).

Biomechanical Analysis

There were no significant differences for torsional stiffness across the 3 groups, although the intact tether group did demonstrate the largest magnitude of torsional stiffness (Figure 7A). For lateral bending stiffness, the control and tether-removed groups were similar in magnitude, and both were statistically lower than the tethered lateral bending stiffness ($P = 0.002$). Stiffness in flexion/extension was significantly lower for the tether-removed group compared with the tethered group ($P = 0.03$), however, there was no statistical difference between either of these groups and the control group.

The total range of motion between the end vertebrae was calculated for each plane of motion (Figure 7B). In torsion, the control group demonstrated the greatest range of motion and was statistically different than both tether conditions ($P < 0.02$). There was no significant difference for torsional range of motion between the tether conditions, although removing the tether did restore some motion to the spine compared with the tethered condition. For lateral bending, the control group demonstrated significantly greater range of motion compared with the tethered condition ($P \leq 0.001$) but was not different compared with the tether-removed condition. When comparing the tether groups, there was a statistical increase in range of motion after tether removal ($P = 0.006$). For flexion/extension, there were no differences between the control group and the tether-removed condition. However, both of these groups demonstrated significantly increased motion compared with the intact tether condition ($P = 0.04$). The total range of

Figure 5. Collagen gene expression (semiquantitative representation). Values are average \pm standard error. There was a trend toward statistical difference for collagen II between tether right side and control ($P = 0.087$).



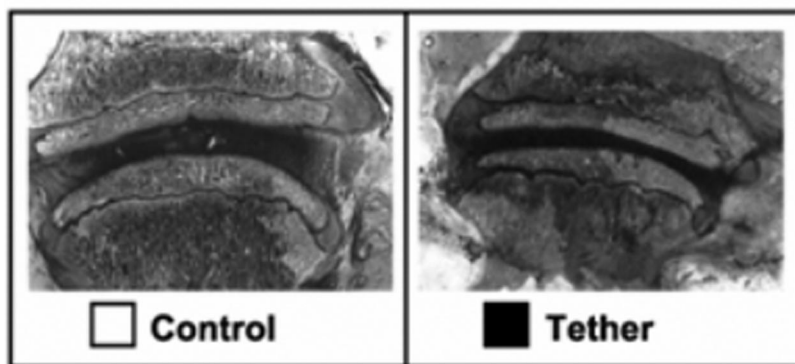
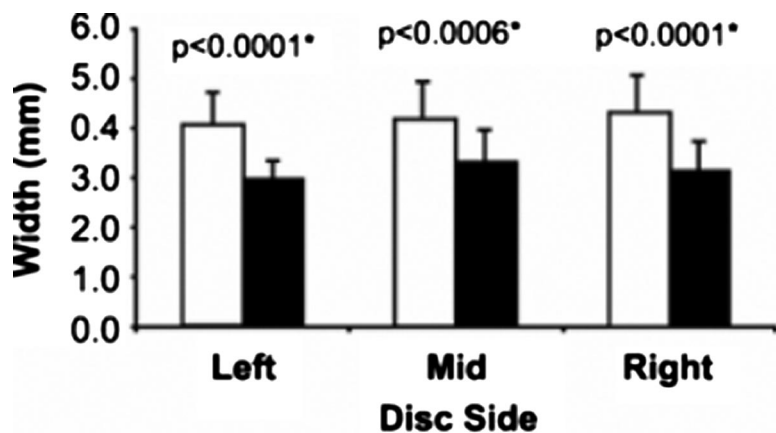


Figure 6. Disc thickness. Values are average \pm standard deviation. Tethered discs were significantly thinner than controls ($P \leq 0.001$ for tethered left, middle, and right sides compared with control). *Statistical significance between groups.

motion between the apical vertebrae in each plane was found to exhibit similar trends when compared with the entire construct (Figure 7C).

Discussion

An anterolateral flexible spinal tether was used in this experimental animal model to create a spinal deformity in a “normal” straight spine. However, the long-term goal of this research would be to provide supporting data to use such a technology in growing patients with scoliosis to correct their deformity. The use of a nonfusion technique in the clinical setting of scoliosis may present unrecognized challenges in obtaining 3-dimensional correction, which was not evaluated in the current model. However, we feel it is critical to understand the effects of spinal growth tethering on the vertebral and disc components of the spinal column before approaching the clinical scenario. The ultimate goals of nonfusion scoliosis correction by growth modulation should not only include spinal realignment, but also, and most importantly, maintain function and mobility of the spine. Therefore, this study evaluated the effects of asymmetric compression on disc health and spinal motion.

Radiographic analysis in this study confirmed the creation of a coronal and sagittal plane spinal deformity over the 6-month growth period. The double tether construct provided appropriate fixation in the vertebral bodies and consistently created notable vertebral wedging compared with controls. In addition, histologic analysis

confirmed that a fusion mass did not develop between adjacent vertebrae, and that all growth plates remained visible. These data seem to indicate that the observed deformity was caused by a compression effect on the growth plate, as described by the Hueter-Volkman law. The compressive forces, passively generated by the tether as spinal length increased, likely caused changes in vertebral growth cartilage function causing decreased growth on the tethered side of the spine. It is important to note that these calf vertebral bodies elongated, on average 9 to 10 mm each over the 6-month study period. Since human adolescent vertebral bodies are known to grow by just over 1 mm per vertebral level per year,²⁶ the effect of growth modulation observed in calves may over estimate the amount of deformity correction possible during the human growth spurt. Future studies using tether implants in adolescent patients are necessary; however, before these studies can be justified, the effect of the tether on the spine and intervertebral discs should be further evaluated in animal models.

Vertebral and intervertebral disc wedging from fusionless spinal growth modulation has been reported previously in other animal studies. Posterolateral tethering resulted in an average of 11.3° of apical wedging (apical disc with 2 adjacent vertebral bodies) after 13 weeks in a goat model; however, the contribution of intervertebral disc wedging was not specifically noted.¹³ In a previous study using the bovine model, single vertebral levels were tethered for a duration of 3

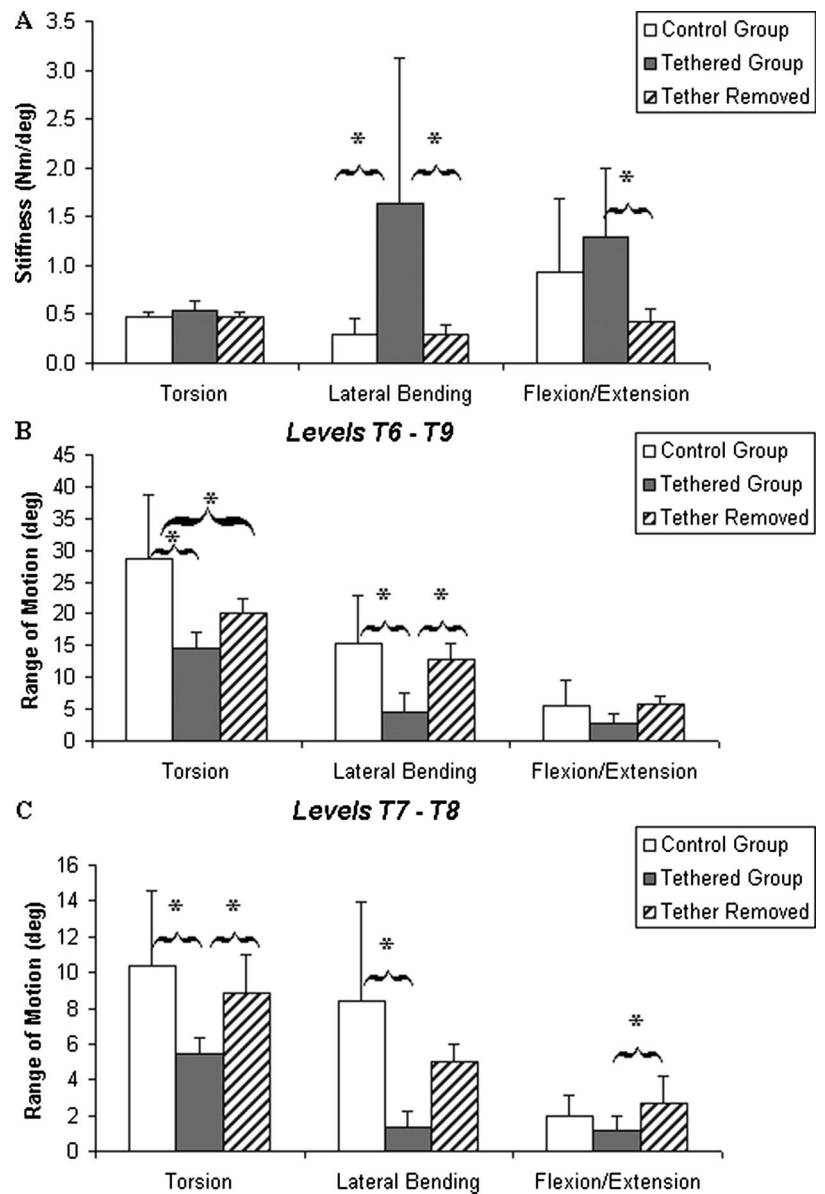


Figure 7. Biomechanical testing data. **A**, Stiffness measurements in torsion, lateral bending, and flexion/extension. **B**, Range of motion measurements between end vertebrae (T6–T9) in torsion, lateral bending, and flexion/extension. **C**, Range of motion measurements between apical vertebrae (T7–T8) in torsion, lateral bending, and flexion/extension. *Statistical significance between groups ($P < 0.05$).

months, and significant intervertebral disc wedging was noted in the tethered ($6.8^\circ \pm 1.6^\circ$) when compared with the untethered ($0.7^\circ \pm 2^\circ$) segments ($P < 0.001$).¹⁵ In the current study, disc thickness decreased almost 30% during the 6 months of tethering; however, disc wedging did not occur.

The rodent-tail model has been used recently to study mechanically accelerated intervertebral disc degeneration. Mechanical loading is thought to alter messenger ribonucleic acid expression and enzyme activation leading to compositional and structural changes in the disc. Specifically, static compression of the disc has been found to result in altered water and proteoglycan content, changes in the architecture of the annulus fibrosus, and changes in biosynthesis and cellular apoptosis.^{27,28} These data correlate with clinical findings of abnormal adjacent segment stresses and disc degeneration in patients treated with long posterior instrumentation and

limited apical fusion. However, in this animal study, gross morphologic and histologic evaluation of the intervertebral discs revealed minimal degenerative changes after 6-months of tethering. Our findings signify the hypothesized advantage of flexible growth modulating constructs, as continued spinal motion is thought to maintain disc health.

Although disc water content was not affected by tethering, further analyses showed alterations in some biochemical parameters. In the tethered tissues, both right and left sides, proteoglycan synthesis rates were increased over control rates. This upregulation of proteoglycan synthesis certainly suggests viability of the chondrocytes within the disc and may represent an attempt by the disc to resist compression. Collagen gene expression was also altered after surgical intervention particularly in the Tether Group on the right (or compressed) side where types II and X collagens appeared to be upregu-

lated. This might reflect an effect of mechanical forces on cells to express a more chondrocytic and/or hypertrophic phenotype.

In prior studies of disc degeneration, the anatomic changes associated with disc degeneration resulted in decreased flexibility²⁹ and loss of swelling pressure.³⁰ Biomechanical analysis was performed in this study to evaluate the flexibility of the spine without tethering, after 6 months of tethering, and after the tether was released. Although the tethered spines did have increased stiffness and decreased motion, after removal of the tether, the spines had very similar motion to those that had not been tethered at all. Despite disc narrowing, the biomechanical data from this study do not indicate that the discs experienced degenerative changes that effected functional motion. Unlike other models of disc degeneration caused by applied compressive forces,^{31,32} the compressive force on the discs in this study developed gradually over 6 months. Additionally, motion, although limited particularly in lateral bending, was maintained at greater than 50% normal. It is postulated that this degree of maintained motion was sufficient to allow the biologic functions of the disc to be largely maintained.

Several limitations of this animal model have to be considered when evaluating this data. Primarily, differences in mechanical forces on the spine, secondary to postural differences between a quadruped bovine and a bipedal human, may affect the ability for spinal growth modulation. In addition, the extremely rapid growth observed in the bovine enabled the creation of a deformity that may not be possible in an adolescent. Perhaps, another animal model that more closely approximates human vertebral growth rates can be used in future studies. Finally, evaluation of disc health was performed in this study after only 6 months of growth modulation, while these tethers would be in place in adolescents for many years before reaching skeletal maturity. The effect of a long-term compressive load and motion limitation on disc health will need to be studied.

There is great interest in identifying a method of controlling progressive scoliosis that will allow and maintain spinal motion. Clinically, this is presently being attempted at some centers with a staple that bridges the disc space and vertebral endplates. The principles of anterior convex compression are similar to those proposed by flexible tethering. The results reported by Betz *et al*³³ suggest an ability to effect spinal growth although in concept a device designed to permit motion while maintaining bony purchase (such as a flexible tether) may be a more ideal approach in the long term. In this study, we have demonstrated that an anterolateral flexible tether can be used to manipulate growth and change the shape of a spine, while maintaining near normal mobility and disc viability. Before this internal brace technology is used in growing children for the correction of idiopathic scoliosis, further testing needs to be done in an animal model that more closely resembles adolescent spinal growth.

■ Key Points

- Six months of anterolateral tethering in a rapidly growing calf spine created significant deformity and vertebral body wedging in the coronal and sagittal planes without causing intervertebral disc wedging.
- Flexible tethering did not result in disc dehydration or gross morphologic degeneration.
- Disc height was decreased and changes in proteoglycan synthesis and collagen type distribution were observed.
- Tethers restricted motion in lateral bending away from the tether and in flexion/extension without limiting torsional motion, however, all motion returned to normal values after tether removal.

Acknowledgments

The authors thank and recognize Stefan Parent, MD, PhD and Gary S. Shapiro, MD for their assistance with surgical procedures, Richard S. Oka, MS for biomechanical testing and analysis, Tracey P. Bastrom, MA for statistical analysis and Michelle Wedemeyer, BS; Tucker Tomlinson, BS; Megan Anderson, MD; and Troy J. Swimmer, BS, for surgical and technical assistance.

References

1. Roaf R. Vertebral growth and its mechanical control. *J Bone Joint Surg Br* 1960;42-B:40–59.
2. Roaf R. The basic anatomy of scoliosis. *J Bone Joint Surg Br* 1966;48:786–92.
3. Miller JA, Nachemson AL, Schultz AB. Effectiveness of braces in mild idiopathic scoliosis. *Spine* 1984;9:632–5.
4. Noonan KJ, Weinstein SL, Jacobson WC, et al. Use of the Milwaukee brace for progressive idiopathic scoliosis. *J Bone Joint Surg Am* 1996;78:557–67.
5. Cochran T, Nachemson A. Long-term anatomic and functional changes in patients with adolescent idiopathic scoliosis treated with the Milwaukee brace. *Spine* 1985;10:127–33.
6. Danielsson AJ, Cederlund CG, Ekholm S, et al. The prevalence of disc aging and back pain after fusion extending into the lower lumbar spine. A matched MR study twenty-five years after surgery for adolescent idiopathic scoliosis. *Acta Radiol* 2001;42:187–97.
7. Hilibrand AS, Robbins M. Adjacent segment degeneration and adjacent segment disease: the consequences of spinal fusion? *Spine J* 2004;4:190S–194S.
8. Park P, Garton HJ, Gala VC, et al. Adjacent segment disease after lumbar or lumbosacral fusion: review of the literature. *Spine* 2004;29:1938–44.
9. Dickson RA, Lawton JO, Archer IA, et al. The pathogenesis of idiopathic scoliosis. Biplanar spinal asymmetry. *J Bone Joint Surg Br* 1984;66:8–15.
10. Piggott H. Growth modification in the treatment of scoliosis. *Orthopedics* 1987;10:945–52.
11. Betz RR, Kim J, D'Andrea LP, et al. An innovative technique of vertebral body stapling for the treatment of patients with adolescent idiopathic scoliosis: a feasibility, safety, and utility study. *Spine* 2003;28:S255–65.
12. Smith AD, Von Lackum WH, Wylie R. An operation for stapling vertebral bodies in congenital scoliosis. *J Bone Joint Surg Am* 1954;36:342–8.
13. Braun JT, Hoffman M, Akyuz E, et al. Mechanical modulation of vertebral growth in the fusionless treatment of progressive scoliosis in an experimental model. *Spine* 2006;31:1314–20.
14. Newton PO, Faro FD, Farnsworth CL, et al. Multilevel spinal growth modulation with an anterolateral flexible tether in an immature bovine model. *Spine* 2005;30:2608–13.
15. Newton PO, Fricka KB, Lee SS, et al. Asymmetrical flexible tethering of spine growth in an immature bovine model. *Spine* 2002;27:689–93.
16. Braun JT, Ogilvie JW, Akyuz E, et al. Experimental scoliosis in an immature goat model: a method that creates idiopathic-type deformity with minimal violation of the spinal elements along the curve. *Spine* 2003;28:2198–203.

17. Thompson JP, Pearce RH, Schechter MT, et al. Preliminary evaluation of a scheme for grading the gross morphology of the human intervertebral disc. *Spine* 1990;15:411-5.
18. Emmanuel J, Hornbeck C, Bloebaum RD. A polymethyl methacrylate method for large specimens of mineralized bone with implants. *Stain Technol* 1987;62:401-10.
19. Sanderson C, Kitabayashi LR. Parallel experience of two different laboratories with the initiator perkadox 16 for polymerization of methylmethacrylates. *J Histotechnol* 1994;17:343-8.
20. Bloebaum RD, Merrell M, Gustke K, et al. Retrieval analysis of a hydroxyapatite-coated hip prosthesis. *Clin Orthop* 1991;267:97-102.
21. Weidner N, Rice DT. Intervertebral disk material: criteria for determining probable prolapse. *Hum Pathol* 1988;19:406-10.
22. Nerlich AG, Schleicher ED, Boos N. Volvo Award winner in basic science studies. Immunohistologic markers for age-related changes of human lumbar intervertebral discs. *Spine* 1997;22:2781-95.
23. Goldman S, Olajos M, Morkin E. Control of cardiac output in thyrotoxic calves. Evaluation of changes in the systemic circulation. *J Clin Invest* 1984;73:358-65.
24. Harper SB, Hurst WJ, Ohlsson-Wilhelm B, et al. The response of various hematologic parameters in the young bovine subjected to multiple phlebotomies. *Asaio J* 1994;40:M816-25.
25. Gay R, Lee RW, Appleton C, et al. Control of cardiac function and venous return in thyrotoxic calves. *Am J Physiol* 1987;252:H467-73.
26. Wever DJ, Tonseth KA, Veldhuizen AG, et al. Curve progression and spinal growth in brace treated idiopathic scoliosis. *Clin Orthop Relat Res* 2000:169-79.
27. Iatridis JC, Mente PL, Stokes IA, et al. Compression-induced changes in intervertebral disc properties in a rat tail model. *Spine* 1999;24:996-1002.
28. Lotz JC. Animal models of intervertebral disc degeneration: lessons learned. *Spine* 2004;29:2742-50.
29. An HS, Anderson PA, Haughton VM, et al. Introduction: disc degeneration: summary. *Spine* 2004;29:2677-8.
30. Stokes IA, Iatridis JC. Mechanical conditions that accelerate intervertebral disc degeneration: overload versus immobilization. *Spine* 2004;29:2724-32.
31. Lotz JC, Chin JR. Intervertebral disc cell death is dependent on the magnitude and duration of spinal loading. *Spine* 2000;25:1477-83.
32. Lotz JC, Hsieh AH, Walsh AL, et al. Mechanobiology of the intervertebral disc. *Biochem Soc Trans* 2002;30(Pt 6):853-8.
33. Betz RR, D'Andrea LP, Mulcahey MJ, et al. Vertebral body stapling procedure for the treatment of scoliosis in the growing child. *Clin Orthop Relat Res* 2005:55-60.